

UC San Diego

UC San Diego Electronic Theses and Dissertations

Title

Soft Tactile Sensing and Interface Design

Permalink

<https://escholarship.org/uc/item/5m54q86m>

Author

Hsiao, Jen-Hsuan

Publication Date

2021

Peer reviewed|Thesis/dissertation

UNIVERSITY OF CALIFORNIA SAN DIEGO

Soft Tactile Sensing and Interface Design

A thesis submitted in satisfaction of the
requirements for the degree of Master of Science

in

Engineering Sciences (Mechanical Engineering)

by

Jen-Hsuan Hsiao

The committee in charge:

Professor Michael Tolley, Chair
Professor Nicholas Boechler, Co-Chair
Professor Tania Morimoto

2021

Copyright

Jen-Hsuan Hsiao, 2021

All rights reserved.

The Thesis of Jen-Hsuan Hsiao is approved, and it is acceptable in quality and form for publication on microfilm and electronically.

University of California San Diego

2021

DEDICATION

For my family.

TABLE OF CONTENTS

THESIS APPROVAL PAGE.....**iii**

DEDICATION **iv**

TABLE OF CONTENTS.....**v**

LIST OF FIGURES..... **vi**

ACKNOWLEDGEMENTS **vii**

ABSTRACT OF THE THESIS.....**viii**

Chapter I : Estimation of object stiffness using variable stiffness soft tactile sensor **1**

 Introduction **2**

 Design **5**

 Design and System Configuration **5**

 Image Processing Pipeline **6**

 Analytical Model **8**

 Stiffness estimation principal: parallel spring model..... **8**

 Sensor stiffness estimation: pneumatic spring model..... **9**

 Results **11**

 Conclusions and Future Work..... **13**

Chapter II : Data-Driven Computational Design of Variable Stiffness Human-Exoskeleton Interface **14**

 Introduction **15**

 Model **17**

 Results **21**

 Conclusions and Future Work..... **23**

Bibliography **24**

LIST OF FIGURES

Figure 1: The stiffness of the variable stiffness tactile sensor is tuned by adjusting the pressure inside the air-tight chamber using a syringe. The input from the depth camera and the pressure sensor are recorded for calculating the stiffness of the object. (a) System setup. (b) Working principle of the variable stiffness soft tactile sensor.	4
Figure 2: Image processing workflow for the depth camera data: from (a) importing raw depth data, (b) defining boundary condition, (c) visualization, (d) filling missing values, (e) coordinate transformation, (f) smoothing, to (g, h) using active contour control to find the contact area between the membrane and the object.	6
Fig . 3: Schematic explaining the equivalence of the setup to a parallel spring model.	8
Figure 4: Theoretical deformation ratio vs. stiffness ratio of object to sensor. The resolution of the sensor is maximized when the deformation ratio is equal to 0.5. This deformation ratio can be achieved if the stiffness of the object is equal to the stiffness of the sensor. Hence, for application of sensors with a wide range of stiffness sensing capability, a variable stiffness sensor is ideal.	9
Figure 5: Stiffness prediction from the sensor and the measurements of the material testing machine.	12
Figure 6: A visual representation of the series spring model applied to the mechanical interfaces of a haptic glove exoskeleton presented in previous work [27].	17
Figure 7: 3D printed silicone samples that mimic the hand dorsum layer and the wearable interface layer shown in the visual representation of series spring model in Figure 6.	19
Figure 8: Elastic modulus of the samples.	19
Figure 9: Simulation of the (A) stiffness profile and (B) peak contact profile of the optimized interfaces and the substrate.	20
Figure 10: Experimental setup for static loading testing on optimized interface to lower peak contact pressure.	22
Figure 11: Comparison between the experiment results (top row) and the simulation (bottom row) showed close alignment.	22

ACKNOWLEDGEMENTS

First, I would like to express my special thanks to Professor Tolley for giving me the opportunity to join the Bioinspired Robotics and Design Lab. He has always provided me all the guidance and support for my research projects. Without his persistent help, the goal of this project would not have been realized.

Besides my advisor, I would like to thank the rest of my committee members: Professor Nicholas Boechler and Professor Tania Morimoto, for their insightful comments and suggestions on my research and thesis.

Additionally, I would like to thank all the collaborators from Creare LLC. They were very helpful for giving the suggestions during the design process and experimental setup of the Human-Exoskeleton interface project.

My sincere thanks also goes to Benjamin Shih and Saurabh Jadhav, the co-authors, for mentoring and guiding me all the ways through different research projects. Further, I would like to thank all the members from the Bioinspired Robotics and Design Lab for supporting and encouraging me all the time. Without each of you, I won't be able to finish the project and the thesis.

This thesis is coauthored with Jen-Hsuan Hsiao, Benjamin Shih, and Saurabh Jadhav. The thesis author was the primary author of this work.

ABSTRACT OF THE THESIS

Soft Tactile Sensing and Interface Design

by

Jen-Hsuan Hsiao

Master of Science in Engineering Sciences (Mechanical Engineering)

University of California San Diego, 2021

Professor Michael Tolley, Chair

Exoskeletons, wearables devices, and prosthetics are all devices that can augment human mobility. Researchers have focused on different aspects from design, materials, control systems, manufacturing techniques, and human study in order to improve the performance of these devices. One of the challenges we are particularly interested in is when pressure concentrations lead to discomfort; how can we address that from a mechanical and materials perspective. In this thesis, we addressed two problems. The first one is related to improving the sensor performance in terms of the range of stiffness sensing. The second one is how changing the material properties in a series spring model could redistribute the contact pressure on the interface.

In the first sensor project, we hypothesized that the range of stiffness sensing could be increased by tuning the sensor stiffness and presented an approach to change the stiffness of the sensor. For our sensor design, we used a depth camera and a pressure sensor to capture deformation and stress on the surface of contact. We tested the stiffness of five different objects, and the estimation error was 8.7%.

In the second part of the thesis, we investigated how tuning the material stiffness could minimize peak contact pressure in static loading conditions. One of the major challenges with exoskeletons and wearables devices is the interface between the wearables and the human user. Pressure concentrations often cause discomfort and thus limit the usability of the exoskeleton for longer durations. We proposed a method to design and fabricate compliant wearable interfaces that users can place between their body and a rigid exoskeleton to achieve design objectives such as redistributing the forces applied to the body by the exoskeleton and thus improve comfort. With our approach, users can analyze the effect of varying the stiffness of the interface on the static responses, lowering the peak contact pressure to reduce pressure concentrations.

Chapter I : Estimation of object stiffness using variable stiffness soft tactile sensor

1. Introduction

Humans can perform dexterous manipulation with their hands, and the fingertips have a high density of morphologically distinct mechanoreceptors that sense and provide different information for our feedback control systems [1]. Previous work has taken inspiration from nature and used different sensing mechanisms to develop tactile sensors.

A flexible capacitive sensor was developed using polydimethylsiloxane (PDMS) as base material and consisted of four capacitors in one unit [2]. The capacitors were arranged in a square such that they could differentiate different types of contact forces (normal force and shear force). Another notable soft pressure sensor designed with the choice of conductive liquid eutectic gallium-indium (eGaIn) that was made using a fabrication process similar to that used to manufacture soft microfluidic devices [3]. The eGaIn was injected in microchannels, embedded in silicon rubber. The hyperelasticity of the rubber made the sensor both soft and stretchable. Bira et al. transformed the change of electric resistance of the eGaIn into a map of tissue stiffness [4]. Studies of how humans perceive differences in compliance also led to the development of a biomimetic tactile sensor [5].

Chorley et al. [6] built a tactile sensor (TacTip) inspired by the layered macro-structure of a fingertip, unlike previous works, Chorley et al. chose to use a 2D camera and traced the surface deflection of the rubber skin. The sensor had a two-point discrimination distance of 5 mm and force sensitivity of 0.05 N. Later work on the TacTip focused on combining tactile perception and robotic actuation to explore edges and surface features [7]. GelSight is another tactile sensor that used a camera to provide high spatial resolution [8], [9]. Follow-on work developed GelSlim with a more compact integration than its predecessor using mirror reflections to change the optical path [10]. Besides 2D camera, Time-of-Flight depth sensor was also used in the development of optical tactile sensor [11]. While depth sensors provide high spatial resolution, they also required more sophisticated calibration when compared to a standard 2D camera.

Most of the published work on tactile sensors has relied on the assumption that both the sensor and the object are elastic and thus, they use a spring model to estimate material characteristics such as the

stiffness of the object. However, when sensing objects with different stiffnesses, Hasegawa et al. observed estimation error became of a large discrepancy in the stiffnesses of the target object and the sensor [12]. This discrepancy also limits the effective range of stiffness sensing. In order to increase the effective sensing range and reduce estimation error, we hypothesize that incorporating a mechanism to change the stiffness of the sensor will help to achieve this goal.

The sensor built for this project is composed of an airtight chamber and an elastic membrane (Figure 1). Changing the pressure of the pneumatic chamber will enable us to change the effective stiffness of the sensor. We estimate the stiffness of the object through the analysis of the depth image of the membrane and the pressure reading of the pneumatic chamber.

The main contributions of this work are:

1. The Development of a variable stiffness sensor that can induce and measure small deformations of a soft object.
2. Propose a framework that utilizes depth data and pressure data to estimate object stiffness.
3. Analyze the assumptions of the contact mechanism for estimating object stiffness and present a pneumatic variable stiffness sensor to increase the range of stiffness sensing.

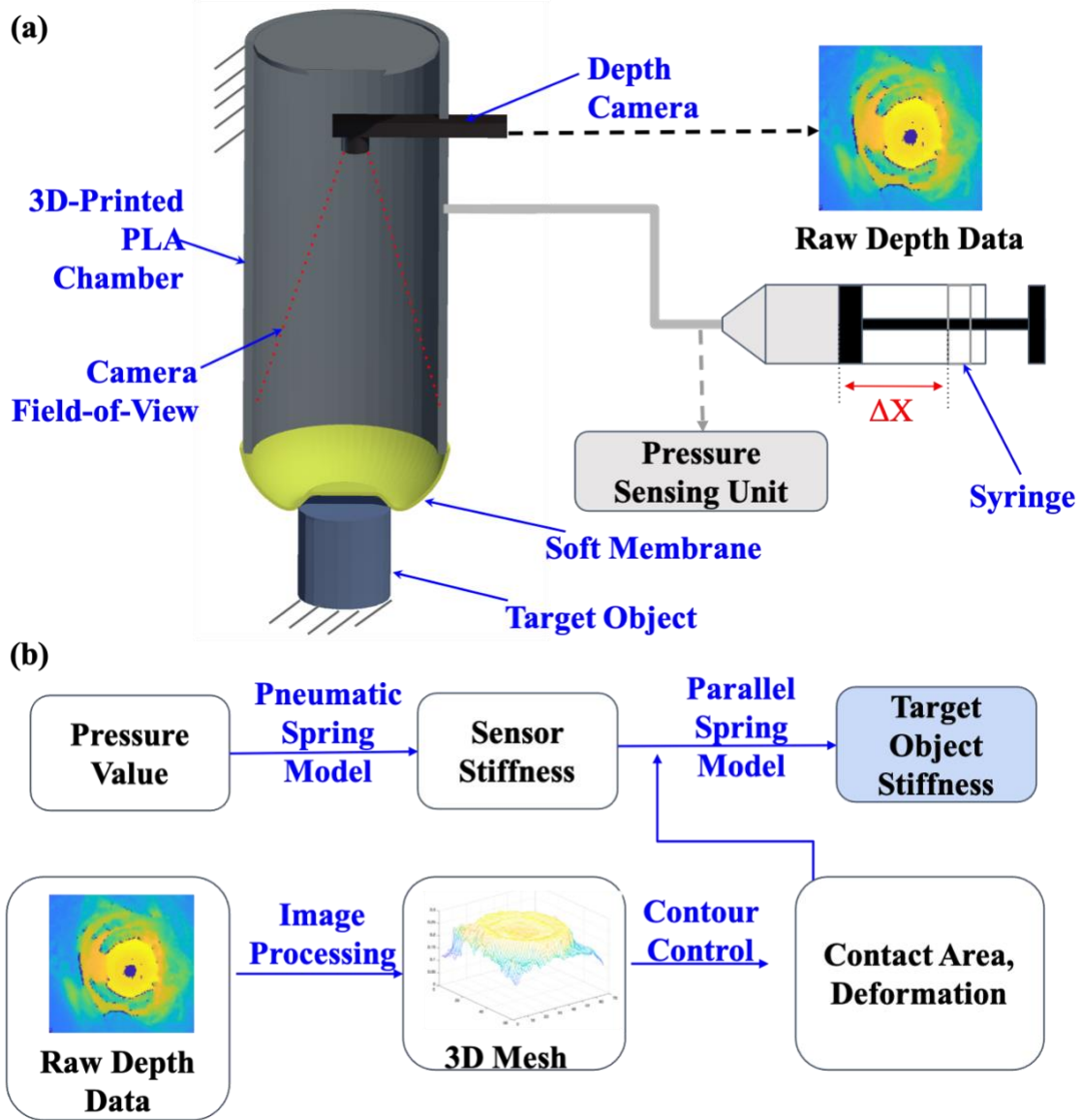


Figure 1: The stiffness of the variable stiffness tactile sensor is tuned by adjusting the pressure inside the air-tight chamber using a syringe. The input from the depth camera and the pressure sensor are recorded for calculating the stiffness of the object. (a) System setup. (b) Working principle of the variable stiffness soft tactile sensor.

2. Design

2.1. Design and System Configuration

Many tactile sensors use a parallel spring model to estimate the stiffness of soft objects with which they interact. To do so, they measure the deflection of both the sensor and the object due to a known applied force. However, there are circumstances when the stiffness of the sensor is not close to the object and hence deformation is dominated by either the sensor, or the object, leading to poor sensitivity. Therefore, we introduce the concept of variable sensor stiffness to increase the effective range of stiffness sensing. The soft tactile sensor built for this project consisted of a spin-coated silicone rubber membrane (Dragon Skin 10, Smooth-On Inc), a 3D printed polylactide (PLA) chamber, a Time-of-Flight depth sensor (CamBoard pico flexx, PMD Technologies) with micrometer-level spatial resolution, a pressure sensor (SSCDANT150PGAA5, Honeywell International Inc), an Arduino Uno microcontroller, and a 200 cc syringe used for adjusting the internal pressure. We performed an indentation experiment to estimate object stiffness from the force-displacement curve. When setting up the experiment, we first gave the sensor an initial pressure and deflection that theoretically set the stiffness of the sensor close to the stiffness of the object and ensure a good contact. The initial applied load and deflection were treated as offset and would later be subtracted from the measurement. Under the current design, the deflection of the syringe was controlled manually. The pressure data and depth data were collected for five seconds and with a frame rate of 45 Hz. The data were sent to Matlab to be processed with image processing pipeline (Figure 2), and we used the result of the image processing pipeline and incorporated the pressure data to estimate the stiffness of the target object.

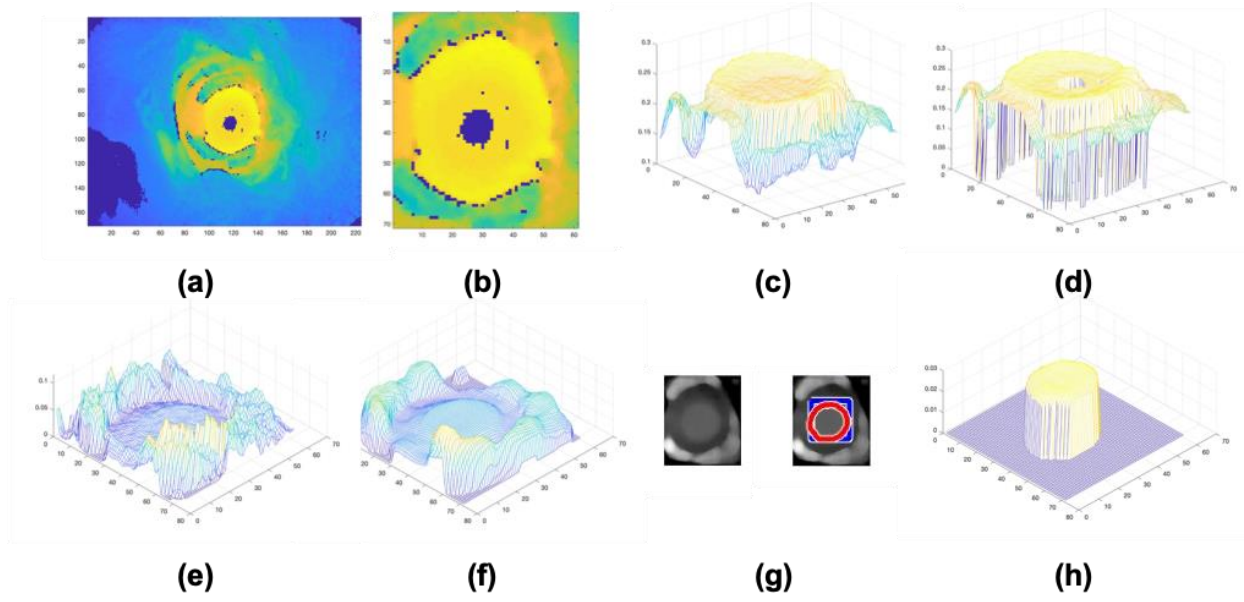


Figure 2: Image processing workflow for the depth camera data: from (a) importing raw depth data, (b) defining boundary condition, (c) visualization, (d) filling missing values, (e) coordinate transformation, (f) smoothing, to (g, h) using active contour control to find the contact area between the membrane and the object.

2.2. Image Processing Pipeline

First, we consider the processing of a single frame. The visualization of the pipeline is shown in Figure 2. Here we use a round sample when developing the pipeline.

- \item Load the raw depth data collected from the ToF depth camera, to be noted, this is in the camera local reference frame.
- \item With the known sensor dimension and constant viewing angle of the ToF depth camera, we can calculate the area the camera covers. The area covers both the membrane and part of the chamber, therefore we need to define the sensing area as the boundary area in this pre-processing stage.
- \item Next, we visualize the raw depth data, and we can see that the blue region in the previous graph is missing data points due to image saturation.
- \item Here, we use a moving median method to fill the missing data points.
- \item After filling the missing points, we then transform the coordinates system from the camera local reference frame to the ground reference frame.
- \item For the noise filtering, we use a 2-D median filtering method to preserve the edge and reduce noise simultaneously.
- \item We perform image segmentation using active contour model to find the contact surface and collect the depth data in that area as our deformation. We first

convert the 3D surface mesh into a binary image and set a blue rectangle mask as our initial guess of the contact area. The active contour control will converge the area of the initial state through expanding or shrinking. Last we apply the converged binary mask to extract data in the contact area, and this is the end of the first frame. \item To process all the data we have, especially for the image segmentation step, we use the converged result from the last frame as the initial mask for the new frame, which is assuming the variance in the contact area is a quasistatic process. \end{enumerate}

3. Analytical Model

3.1. Stiffness estimation principal: parallel spring model

We chose a parallel spring model [13] because it accurately represented our system setup and the simplicity of the control system required. A parallel spring setup (Figure 3) allowed us to use the depth camera to capture the deformation on the surface of contact. When the sensor was in contact with the object, we assumed both the sensor and the testing object were elastic materials and experienced the same amount of deformation when load is applied. The relationship between the applied force F and the deformation X was given by:

$$F = (k_{sensor} + k_{object})\Delta X \quad (1)$$

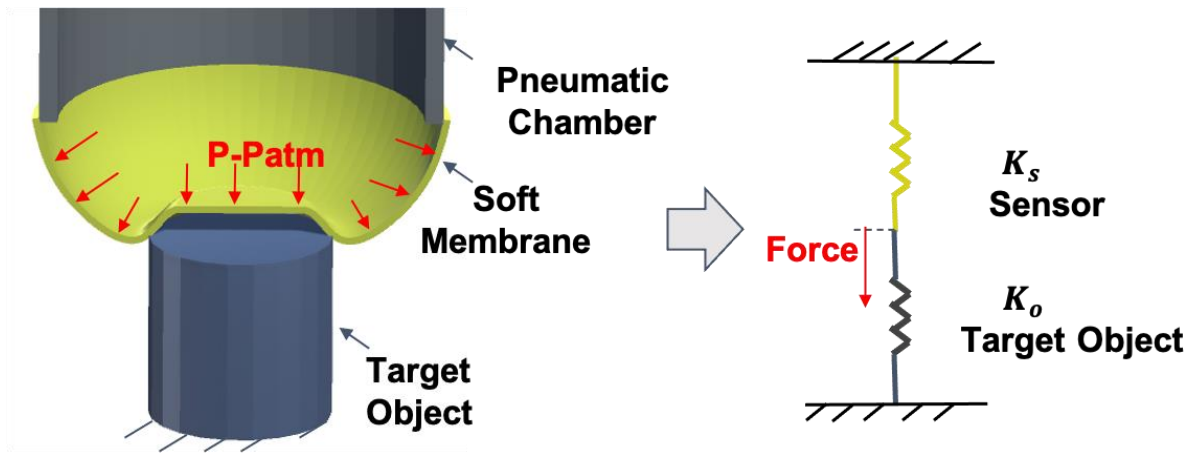


Figure 3: Schematic explaining the equivalence of the setup to a parallel spring model.

When the stiffness of the sensor was close to the target object we sensed a noticeable change in indentation depth and estimate the stiffness of the object through deriving the slope of the force to displacement curve. With a constant force and constant sensor stiffness, the range of stiffness sensing was around $10^{-2} \sim 10^2$ times the sensor stiffness (Figure 4), this range of stiffness ratio covered over 98% of the range of sensor deformation. Any object that is 100 times harder or softer than the sensor stiffness, would only contribute 2% of the range of sensor deformation. Therefore, we hypothesized that by changing

the stiffness of the sensor to make it close to the stiffness of the target object, we would be able to increase the effective range of stiffness sensing where a measurable deformation could be captured and used to estimate object stiffness.

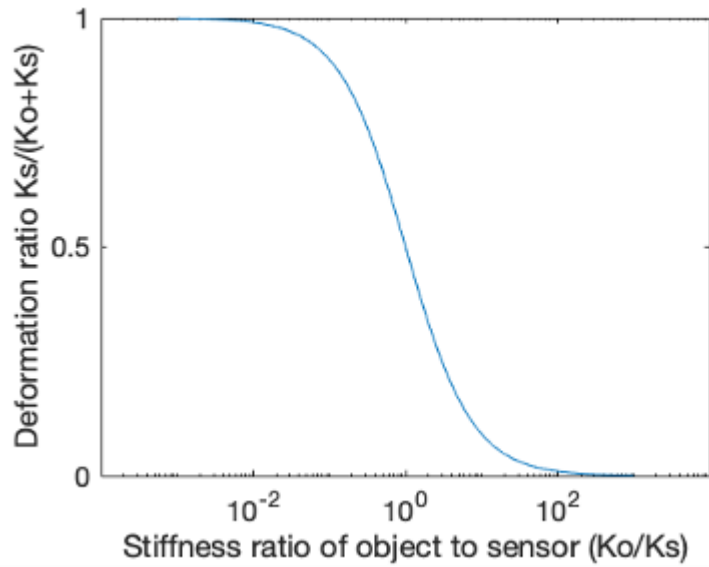


Figure 4: Theoretical deformation ratio vs. stiffness ratio of object to sensor. The resolution of the sensor is maximized when the deformation ratio is equal to 0.5. This deformation ratio can be achieved if the stiffness of the object is equal to the stiffness of the sensor. Hence, for application of sensors with a wide range of stiffness sensing capability, a variable stiffness sensor is ideal.

3.2. Sensor stiffness estimation: pneumatic spring model

While the sensor was modeled as an elastic element, we made the following assumptions when deriving the stiffness of the sensor k :

1. We were only considering the elastic property of the compressible air as a pneumatic spring [14] and neglecting the change of stiffness the membrane contributed.
2. We were also neglecting the change of volume when the membrane was pressurized and inflated. We assumed the volume of the chamber to be constant but not the volume of the syringe throughout the measurement.
3. The gas inside the sensor (chamber and syringe) was ideal.

4. During the measurement, when the internal pressure was increased to generate indentation to the object, such a process was an adiabatic transformation, and no thermal energy was exchanged with the surroundings.
5. An uniform pressure distribution was also assumed on the contact surface, which simplified the force estimation step.
6. The variations of the cross-sectional area of the chamber was assumed to be constant and used to simulate the force delivered by the pneumatic spring.

When consider the compressible air inside the sensor as a pneumatic spring, the stiffness of the pneumatic spring can be found with the definition of $k = \frac{\partial F}{\partial x}$

$$k = \frac{P\gamma A_{chamber}A_{syringe}}{V_{chamber}+(L_0-x)A_{syringe}} \quad (2)$$

Where $V_{chamber}$ is the volume of the chamber, sensor air volume V , internal pressure P , and adiabatic constant γ . The chamber has a cross sectional area $A_{chamber}$, the syringe has a cross sectional area $A_{syringe}$, initial pneumatic spring length L_0 , and deflection x which can range between 0 and L_0 .

4. Results

We molded and tested five samples that had various Young's moduli but the same dimension of $30mm \times 30mm \times 15mm$. The samples were placed right underneath the membrane, and the sensor was given an offset pressure and inflated to ensure full contact with the object, which was similar to the offset step when performing a material test with a material testing machine. After the sensor and the sample are in contact, we applied more pressure by changing the volume of the syringe. The deflection of the syringe was controlled using a open loop control. While the pressure inside the chamber increased and inflated the membrane, we measured the deformation of the membrane with the depth camera. After collected the pressure and deformation data, we found the contact area using the image processing pipeline with active contour control. The integral of the pressure over the contact area gave us the contact force. Similar to the pressure and deformation offset steps, we subtracted the initial contact force. We then got the force-displacement curve from the measured data for the sensor plus sample, and the slope gave us the estimated combined stiffness of the sensor and the sample $k_{sensor} + k_{object}$. We used Eq. 2 to estimate the stiffness of the sensor and subtract this value from the combined stiffness to get the estimated sample stiffness with estimation error of 8.7%. (Figure 5).

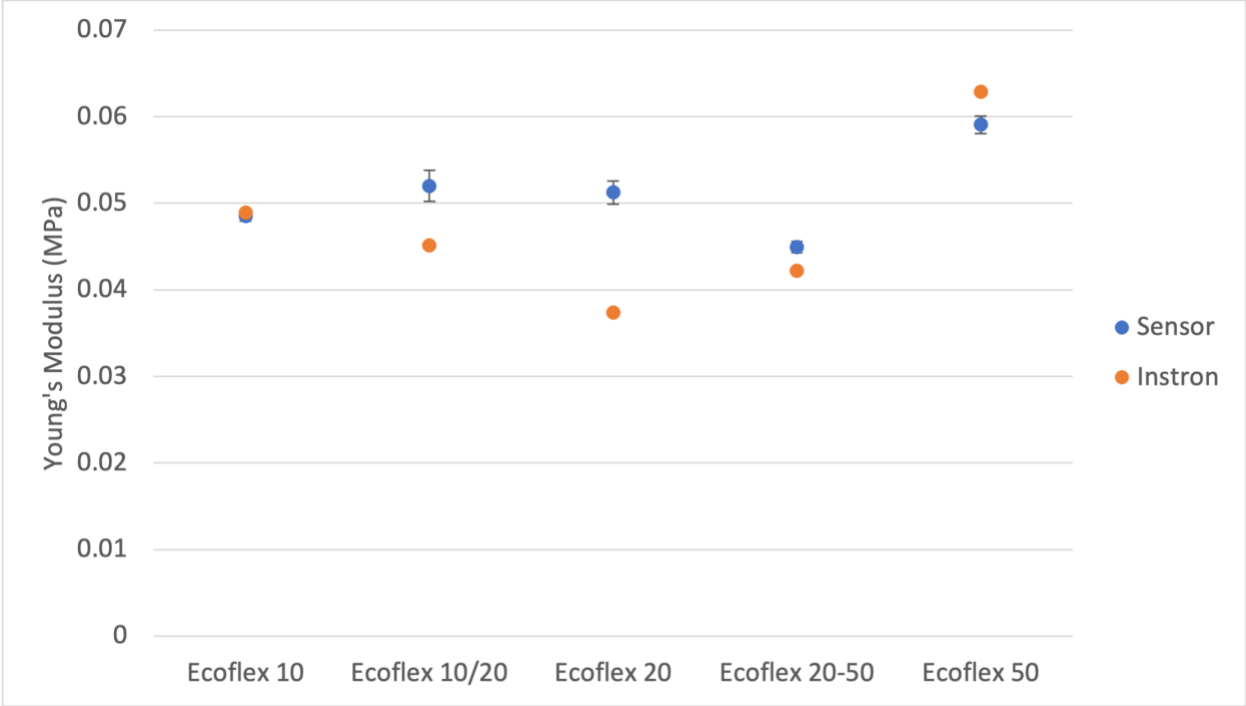


Figure 5: Stiffness prediction from the sensor and the measurements of the material testing machine.

5. Conclusions and Future Work

In this work, we have presented the first sensor capable of object stiffness estimation with adjustable tactile sensor stiffness. The sensor we built for this project has a depth camera embedded in an airtight pneumatic chamber, which we modeled as a pneumatic spring. By adjusting the internal pressure of the air chamber, we were able to change the stiffness of the pneumatic spring, increasing both the upper limit and the lower limit on the range of stiffness sensing. Preliminary test had an estimation error of stiffness of 8.7%. The tests were conducted against target objects with homogeneous material properties, however with the high spatial resolution, such sensor has the potential to create a map of stiffness against composite target object that has non-homogeneous material properties. A main challenge of this application is the portability since tuning the pneumatic pressure of a wide range requires a vacuum machine, therefore sizing down the device to a portable size will be the main focus of our future work.

Future work will focus both on the design, modeling, and control aspects. For the next iteration of the design, we will like to make the sensor into a portable scale as well as test it on a robotic arm for robotic manipulation; for the model of estimating sensor stiffness, we will need to consider the deformation of the membrane as well as the contact mechanics and pressure distribution on the surface of contact which we assumed to be uniform for now; for the control of the system we will like to incorporate differential pressure control as feedback control and real-time filter for the pressure sensor. To reduce the range of error in estimation, we should iterate the entire estimation process until the estimation of object stiffness converges similar to a root finding problem where the pressured value for the sensor is the initial guess. Additionally, our sensor can be incorporated with finite element analysis tool to find material stiffness in objects with complicated shapes. Similarly, we iterate the estimated stiffness profile in finite element analysis until convergence. Last, on the manufacturing end, we will test different materials for the membrane, which relates to the potential image saturation of the depth camera and further improve the sealing for the chamber to withstand higher pressure and thus increase the adjustable range of sensor stiffness plus the range of stiffness sensing.

Chapter II : Data-Driven Computational Design of Variable Stiffness Human-Exoskeleton

Interface

1. Introduction

Exoskeletons are devices worn by the user to fit closely to the human body and move in conjunction with the movement of the body [15], [16]. The design and development of exoskeletons is an active area of research for applications in wearable haptics [17], [18], rehabilitation devices [19], [20], prosthetics [21], and subject-centered robotic suits to augment human capabilities [22]. Previous research has explored increasing the usability and comfort of exoskeletons custom-designed mechanical interfaces that fit the individual's body contours and anatomical needs [23]. However, limited research has been done to explore the effect of the stiffness of the interface on the usability of the exoskeleton.

Designing an exoskeleton to reduce the discomfort for a user is a challenging problem, especially when using a rigid exoskeleton to interface with the skin. Prolonged use of exoskeletons with rigid mechanical interfaces for prosthetics is known to cause wounds and ulcers due to pressure and shear forces at the contact interfaces [24]. Previous exoskeletons with applications in wearable haptics and rehabilitation devices have usually overcome this drawback by embedding the rigid device in fabric or using a soft silicone sleeve between the rigid interface and skin [19, 24]. Functionally graded and variable stiffness structural design has been studied by some researchers and found to be beneficial for minimizing peak contact pressure and stress concentrations in response to certain loading conditions. For example, Kumar et al. [25] investigated the jaws, anchoring hooks of the invertebrates, and found their multi-directional graded structures are not only strong but compliant and resilient at the same time. Kumar et al 3D printed a functionally graded end effector and found it to perform better than pure soft or rigid ones in shear loading test where the graded effector were able to minimize stress concentrations at the joint and maintained its bending stiffness. Sengeh et al. , presented the design of a variable impedance prosthetic socket optimized for comfort using CAD/CAM technology and Magnetic Resonance Imaging data [21]. However, in this work, the inverse proportional relationship between the interface and the human body was only experimentally tested but was discussed in the modeling section. Varghese et al., explored the concept of optimizing the hand exoskeletons for comfort by tuning the stiffness of the exoskeleton design at the

interface [26]. They used an analytical model to optimize the stiffness at the exoskeleton-skin interface and to minimize the peak contact pressure. Their analytical model consisted of a simplified representation of the hand dorsum (soft tissue) and the interface as a two-plate model. However, this work made several assumptions to simplify the calculation such as assuming the boundary conditions like the force and moment as a point load at the center of the plate and assuming the pressure constant along the width of the plate.

2. Model

In our work, we assumed that pressure concentrations would lead to discomfort, and therefore we hypothesized that tuning material stiffness in a series spring model of human-wearable device interaction can minimize peak contact pressure. We combined analytical modeling of a series spring model (Figure 6) with computational tools and finite element analysis (FEA) technology to design and optimize the stiffness profile of the wearable interface between the exoskeleton and the human. In the 2D analytical model, we considered the effects of shear force due to friction at the mechanical interface and the variable pressure along the width of the interface. In the 3D analytical model, we included the out-of-plane force components and incorporated multi-objective optimization for varying locations and magnitudes of the forces. We used this data-driven computational design to test hypotheses related to the performance metrics of the exoskeleton, in particular, we focused on minimizing the peak reaction pressure to improve the comfort of the wearer and tested such hypotheses in our experiment.

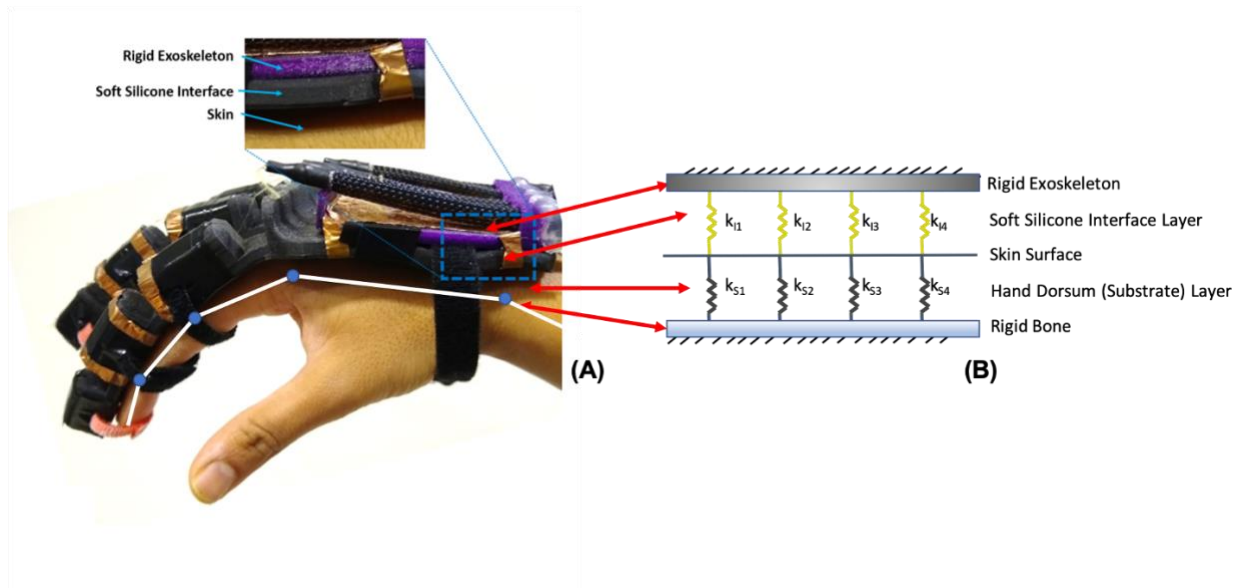


Figure 6: A visual representation of the series spring model applied to the mechanical interfaces of a haptic glove exoskeleton presented in previous work [27]. The actuators used to render force feedback on the fingers are grounded to the rigid exoskeleton attached to the hand with a soft mechanical interface consisting of a silicone layer (A). When applied the proposed variable stiffness design to the interface of the haptic glove to achieve an uniform pressure distribution, we 3D printed different materials at different location to match the stiffness profile of the hand dorsum layer (B).

In the demonstration, we formulated the design objective of minimizing the peak contact reaction pressure of a haptic device (Figure 6). We treated the interface layer (soft silicone interface) and the substrate layer (hand dorsum) as a series spring model whereas the spring constant of the substrate layer is fixed, and we optimized the spring constant of the interface layer to achieve our design objective of minimizing the peak contact pressure on the interface layer. For the stiffness profile of the substrate layer, we used acrylic to mimic the hand bone structure and used soft acrylic to mimic the soft tissue structure of the human body (Figure 7). For the stiffness profile of the interface layer, materials were chosen from ten different materials that can be 3D printed (Figure 8). Since we used acrylic in the center and soft silicone on the side of the substrate sample, the stiffness profile showed a higher value in the center and lower on the side in Figure 9 (A). In order to minimize the peak contact pressure, a root-finding algorithm was used and the stiffness profile of the optimized interface was chosen to have lower stiffness in the middle and higher stiffness on the side which formed an inverse relationship to the stiffness profile of the substrate sample. (Figure 9 (B)).

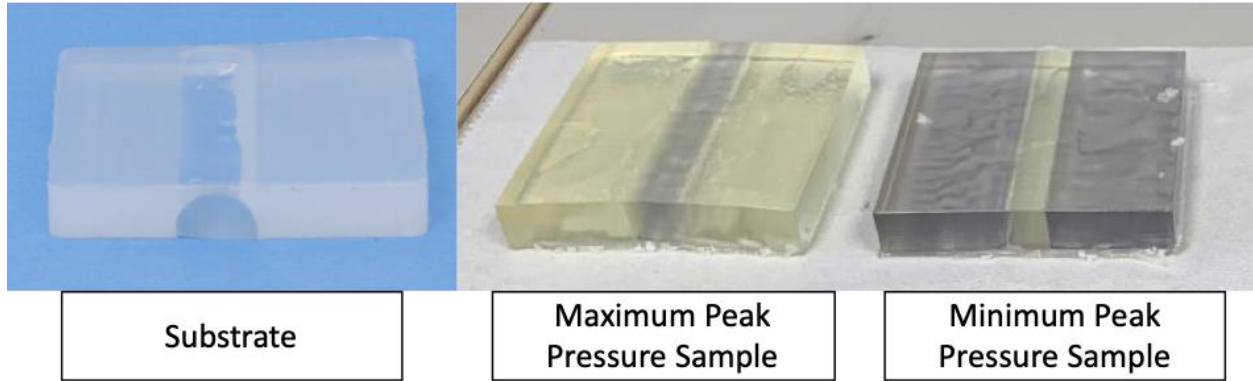


Figure 7: 3D printed silicone samples that mimic the hand dorsum layer and the wearable interface layer shown in the visual representation of series spring model in Figure 6.

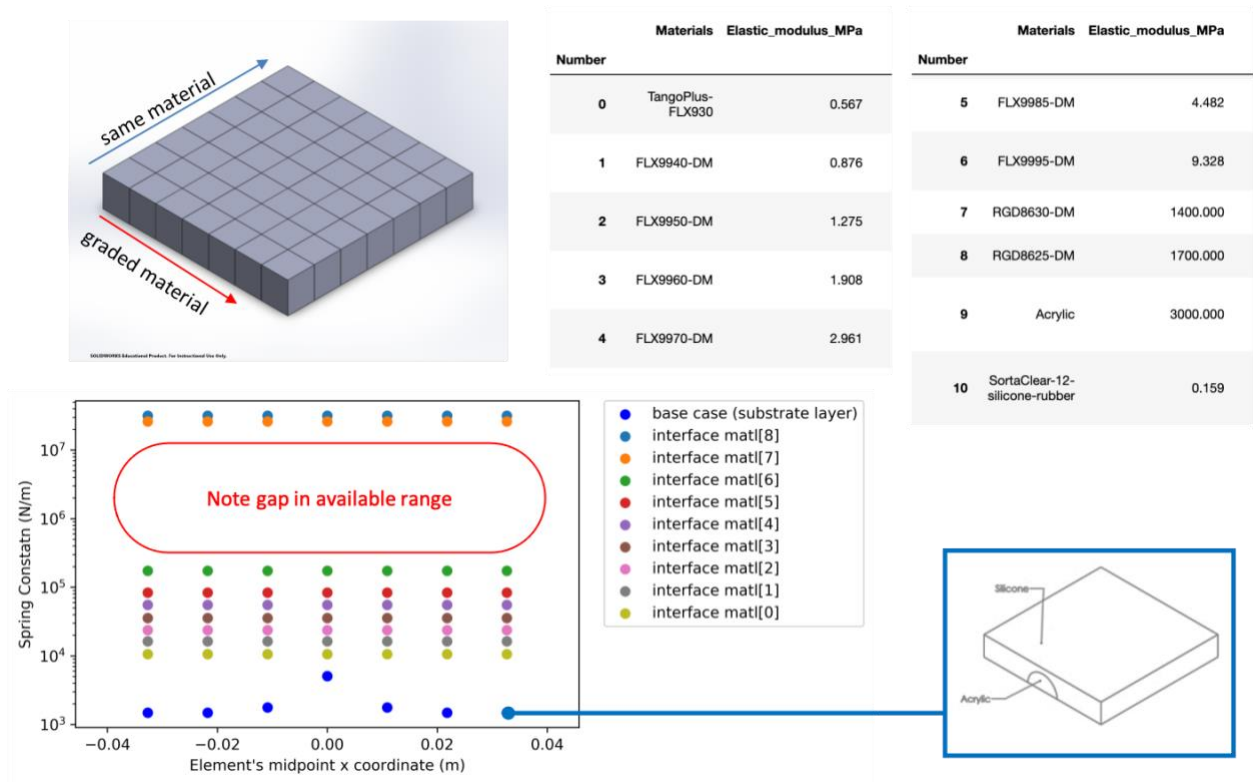


Figure 8: Elastic modulus of the samples.

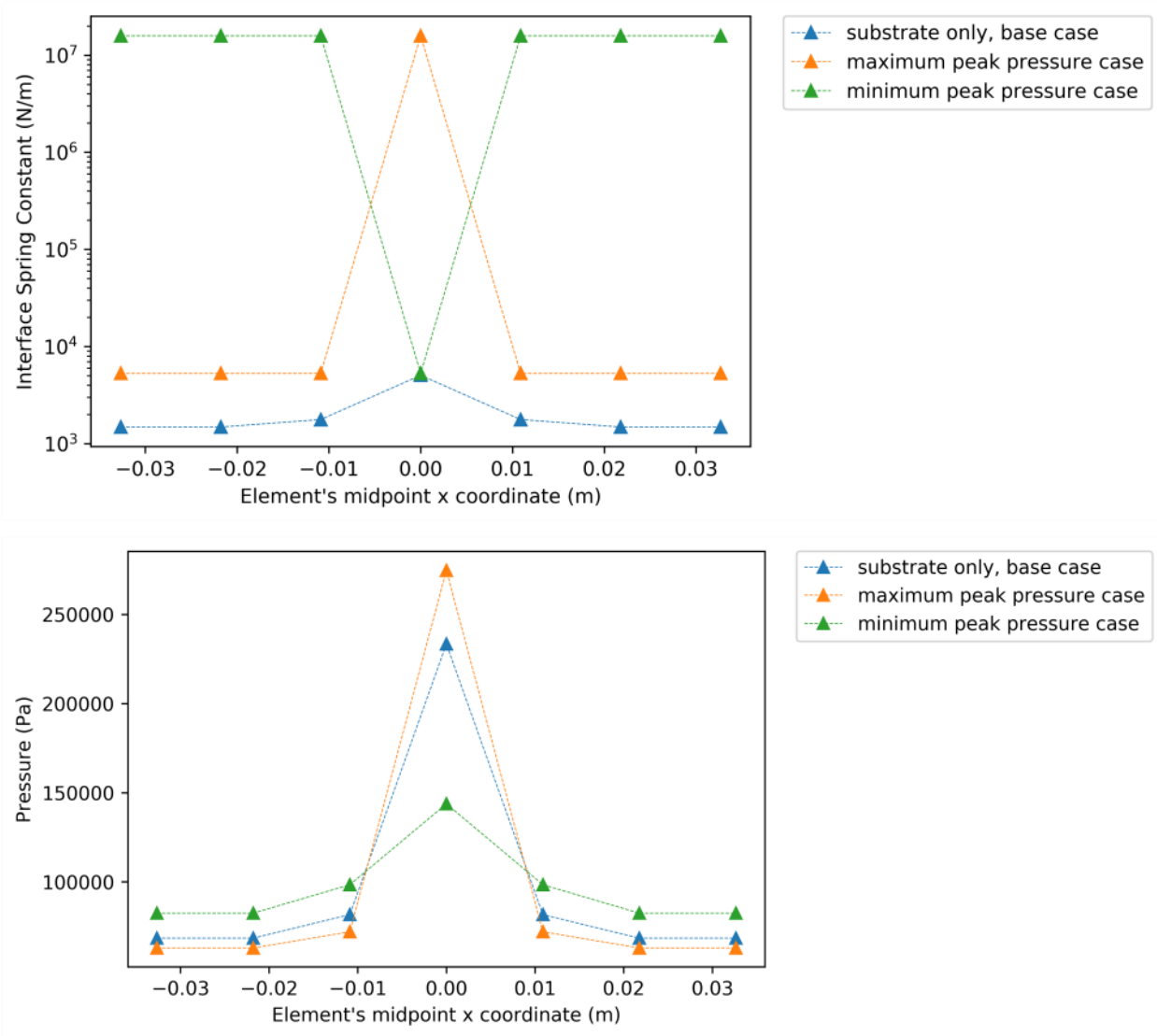


Figure 9: Simulation of the (A) stiffness profile and (B) peak contact profile of the optimized interfaces and the substrate.

3. Results

The objective of this test was to measure the generated contact stresses to an applied load across preselected material interfaces that were designed to minimize the peak contact pressure. In the experiment setup, a load cell was used to applied a 125 lbf force to a rigid plate that was placed on top of the interface layer and the substrate layer (Figure 10). A pressure-sensitive contact film was placed between the material sample and the rigid base plate to collect the data of the pressure distribution on the interface layer.

We will apply a compression load to one face of the interface, and map the pressure contours on the opposite face. The applied load will be measured with a load cell, and the normal stress concentrations will be mapped with pressure-sensitive contact film placed between the material sample and the rigid base plate. Our goal is to test materials with a wide range of material properties ranging from homogeneously soft materials and homogeneously stiff materials. This will be done on different idealized base plate geometries including flat, convex, and concave base plate. Optimum interfaces will minimize stress concentrations on the wearer by distributing loads evenly across the skin contact area. A camera was placed under the substrate layer to record the color change of the pressure sensitive film throughout the experiment. For this demonstration case that mimics the human hand dorsum, from the simulation we saw pressure concentrations in the middle when the load is directly applied to the substrate layer (Figure 11). When the optimized interface is attached to the substrate, we saw a decrease in the peak pressure in the middle when the pressure was redistributed. Inversely, when we attached an interface that has a higher stiffness value in the middle which is similar to the stiffness profile of the substrate, we saw the peak pressure increased from the simulation. We compared the experimental results with the simulation and found a close alignment, the only difference was the pressure concentrations where the stiffness profile showed a discontinuity.

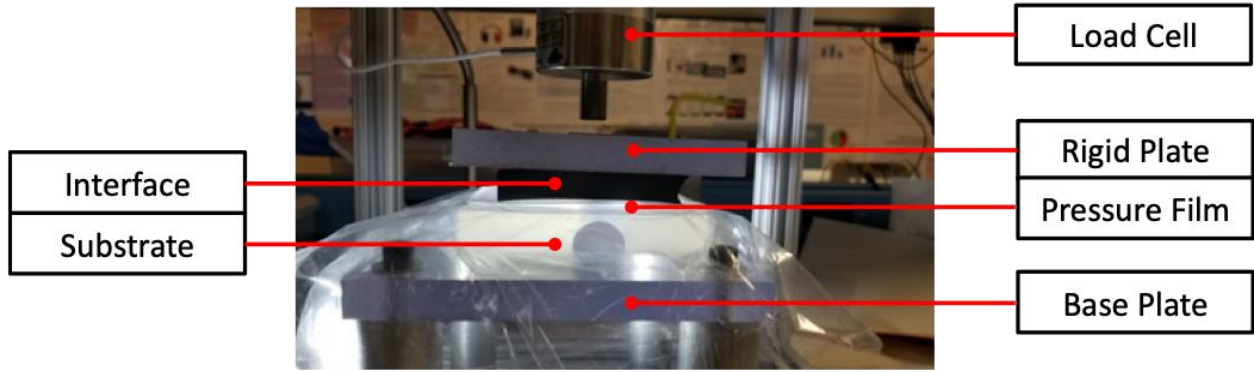


Figure 10: Experimental setup for static loading testing on optimized interface to lower peak contact pressure. Photos and data courtesy of Creare LLC.

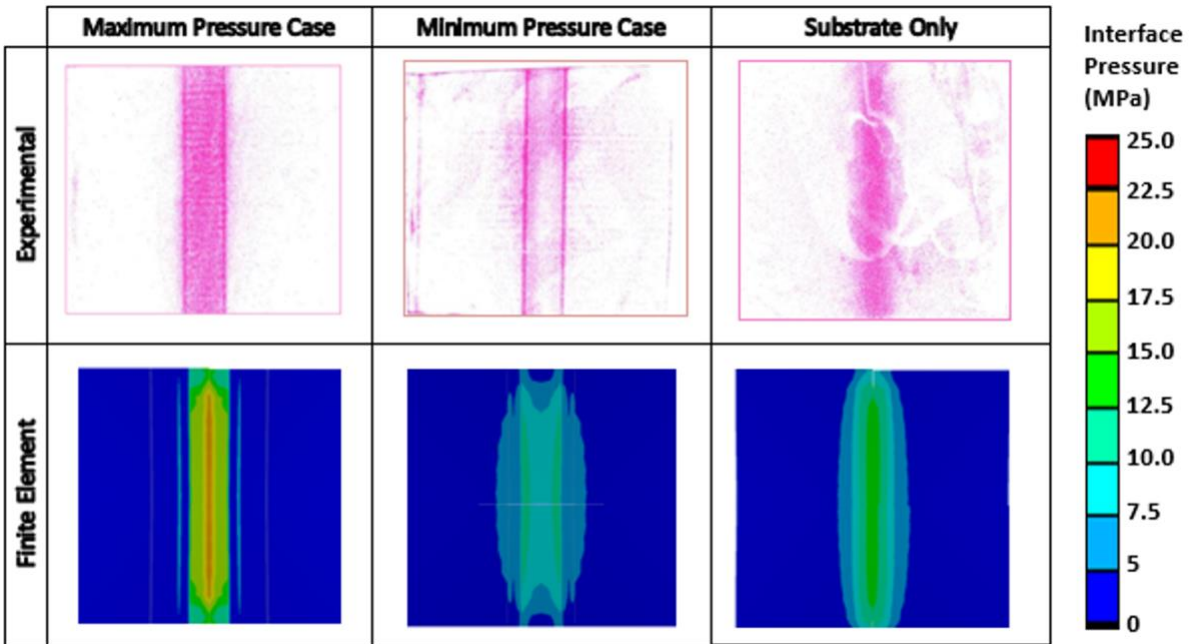


Figure 11: Comparison between the experiment results (top row) and the simulation (bottom row) showed close alignment. Photos and data courtesy of Creare LLC.

4. Conclusions and Future Work

In this work we assumed that pressure concentrations leads to discomfort when having wearable devices on the body. We treated the human body and wearable devices with a series spring model and hypothesized that by tuning the material stiffness in the series spring model we can minimize the peak contact pressure on the interface in static loading. The design of the interface was optimized through implementing a root finding algorithm on the series spring model. A commercial finite element analysis software was also used in simulating the pressure distribution between the interface layer (that represented the wearable device) and the substrate layer (that represented the human body). Samples of the interface and substrate were 3D printed according to the stiffness profile from the optimized spring model simulation. The experimental results showed close alignment to both the optimized model as well as the commercial finite element software. In the future, we plan to investigate and test more complicated loading conditions by adding in out of plane forces and torques, as well as dynamic responses. From the manufacturing perspective, we are also working on tuning material structures to achieve different levels of stiffness when printing the same material to optimize the performance of our interface design.

This thesis is coauthored with Jen-Hsuan Hsiao, Benjamin Shih, and Saurabh Jadhav. The thesis author was the primary author of this work.

Bibliography

1. Purves, D., G. J. Augustine, D. Fitzpatrick, L. C. Katz, A. S. LaMantia, J. O. McNamara, and S. M. Williams. "Mechanoreceptors specialized to receive tactile information." *Neuroscience* (2001).
2. Lee, Hyung-Kew, Jaehoon Chung, Sun-Il Chang, and Euisik Yoon. "Normal and shear force measurement using a flexible polymer tactile sensor with embedded multiple capacitors." *Journal of Microelectromechanical Systems* 17.4 (2008): 934-942.
3. Park, Yong-Lae, Carmel Majidi, Rebecca Kramer, Phillippe Bérard, and Robert J. Wood. "Hyperelastic pressure sensing with a liquid-embedded elastomer." *Journal of micromechanics and microengineering* 20.12 (2010): 125029.
4. Bira, Nicholas, and Yiğit Mengüç. "Measurement of tissue stiffness using soft EGA-in sensors and pressure application." *2018 IEEE International Conference on Soft Robotics (RoboSoft)*. IEEE, 2018.
5. Su, Zhe, Jeremy A. Fishel, Tomonori Yamamoto, and Gerald E. Loeb. "Use of tactile feedback to control exploratory movements to characterize object compliance." *Frontiers in neurorobotics* 6 (2012): 7.
6. Chorley, Craig, Chris Melhuish, Tony Pipe, and Jonathan Rossiter. "Development of a tactile sensor based on biologically inspired edge encoding." *2009 International Conference on Advanced Robotics*. IEEE, 2009.
7. Lepora, Nathan F., Kirsty Aquilina, and Luke Cramphorn. "Exploratory tactile servoing with active touch." *IEEE Robotics and Automation Letters* 2.2 (2017): 1156-1163.
8. Yuan, Wenzhen, Rui Li, Mandayam A. Srinivasan, and Edward H. Adelson. "Measurement of shear and slip with a GelSight tactile sensor." *2015 IEEE International Conference on Robotics and Automation (ICRA)*. IEEE, 2015.
9. Yuan, Wenzhen, Siyuan Dong, and Edward H. Adelson. "Gelsight: High-resolution robot tactile sensors for estimating geometry and force." *Sensors* 17.12 (2017): 2762.
10. Donlon, Elliott, Siyuan Dong, Melody Liu, Jianhua Li, Edward Adelson, and Alberto Rodriguez. "Gelslim: A high-resolution, compact, robust, and calibrated tactile-sensing finger." *2018 IEEE/RSJ International Conference on Intelligent Robots and Systems (IROS)*. IEEE, 2018.
11. Alspach, Alex, Kunimatsu Hashimoto, Naveen Kuppuswamy, and Russ Tedrake. "Soft-bubble: A highly compliant dense geometry tactile sensor for robot manipulation." *2019 2nd IEEE International Conference on Soft Robotics (RoboSoft)*. IEEE, 2019.
12. Hasegawa, Yoshihiro, Mitsuhiro Shikida, Takeshi Shimizu, Takaaki Miyaji, Hikaru Sasaki, Kazuo Sato, and Koichi Itoigawa. "Amicromachined active tactile sensor for hardness detection." *Sensors and Actuators A: physical* 114.2-3 (2004): 141-146.

13. Shikida, Mitsuhiro, Takeshi Shimizu, Kazuo Sato, and Koichi Itoigawa. "Active tactile sensor for detecting contact force and hardness of an object." *Sensors and Actuators A: physical* 103.1-2 (2003): 213-218.
14. Savaresi, Sergio M., Charles Poussot-Vassal, Cristiano Spelta, Olivier Sename, and Luc Dugard. *Semi-active suspension control design for vehicles*. Elsevier, 2010.
15. Herr, Hugh. "Exoskeletons and orthoses: classification, design challenges and future directions." *Journal of neuroengineering and rehabilitation* 6.1 (2009): 1-9.
16. Mohammed, Samer, Yacine Amirat, and Hala Rifai. "Lower-limb movement assistance through wearable robots: State of the art and challenges." *Advanced Robotics* 26.1-2 (2012): 1-22.
17. Gu, Xiaochi, Yifei Zhang, Weize Sun, Yuanzhe Bian, Dao Zhou, and Per Ola Kristensson. "Dexmo: An inexpensive and lightweight mechanical exoskeleton for motion capture and force feedback in VR." *Proceedings of the 2016 CHI Conference on Human Factors in Computing Systems*. 2016.
18. Choi, Inrak, Elliot W. Hawkes, David L. Christensen, Christopher J. Ploch, and Sean Follmer. "Wolverine: A wearable haptic interface for grasping in virtual reality." *2016 IEEE/RSJ International Conference on Intelligent Robots and Systems (IROS)*. IEEE, 2016.
19. Polygerinos, Panagiotis, Kevin C. Galloway, Emily Savage, Maxwell Herman, Kathleen O'Donnell, and Conor J. Walsh. "Soft robotic glove for hand rehabilitation and task specific training." *2015 IEEE international conference on robotics and automation (ICRA)*. IEEE, 2015.
20. Vitiello, Nicola, Tommaso Lenzi, Stefano Roccella, Stefano Marco Maria De Rossi, Emanuele Cattin, Francesco Giovacchini, Fabrizio Vecchi, and Maria Chiara Carrozza. "NEUROExos: A powered elbow exoskeleton for physical rehabilitation." *IEEE transactions on robotics* 29.1 (2012): 220-235.
21. Sengeh, David Moinina, and Hugh Herr. "A variable-impedance prosthetic socket for a transtibial amputee designed from magnetic resonance imaging data." *JPO: Journal of Prosthetics and Orthotics* 25.3 (2013): 129-137.
22. Zhang, Juanjuan, Pieter Fiers, Kirby A. Witte, Rachel W. Jackson, Katherine L. Poggensee, Christopher G. Atkeson, and Steven H. Collins. "Human-in-the-loop optimization of exoskeleton assistance during walking." *Science* 356.6344 (2017): 1280-1284.
23. Pons, José L. *Wearable robots: biomechatronic exoskeletons*. John Wiley & Sons, 2008.
24. Salawu, A., C. Middleton, A. Gilbertson, K. Kodavali, and V. Neumann. "Stump ulcers and continued prosthetic limb use." *Prosthetics and orthotics international* 30.3 (2006): 279-285.
25. Kumar, Kitty, Jia Liu, Caleb Christianson, Mustafa Ali, Michael T. Tolley, Joanna Aizenberg, Donald E. Ingber, James C. Weaver, and Katia Bertoldi. "A biologically inspired, functionally graded end effector for soft robotics applications." *Soft robotics* 4.4 (2017): 317-323.
26. Varghese, Rohit John, Gaurav Mukherjee, Raymond King, Sean Keller, and Ashish D. Deshpande. "Designing Variable Stiffness Profiles to Optimize the Physical Human Robot

Interface of Hand Exoskeletons." *2018 7th IEEE International Conference on Biomedical Robotics and Biomechatronics (Biorob)*. IEEE, 2018.

27. Jadhav, Saurabh, Mohamad Ramzi Abdul Majit, Benjamin Shih, Jürgen P. Schulze, and Michael T. Tolley. "Variable Stiffness Devices Using Fiber Jamming for Application in Soft Robotics and Wearable Haptics." *Soft Robotics* (2021).